Supplementary information

Pharmacomodulation of a ligand targeting the HBV capsid hydrophobic pocket

Mathilde BRIDAY[1], François HALLÉ[2], Lauriane LECOQ*[1], Sylvie RADIX[2], Juliette MARTIN[1], Roland MONTSERRET[1], Marie DUJARDIN[1], Marie-Laure FOGERON[1], Michael NASSAL[3], Beat H. MEIER[4], Thierry LOMBERGET*[2], Anja BÖCKMANN*[1]

[1] Molecular Microbiology and Structural Biochemistry (MMSB) UMR 5086 CNRS/Université de Lyon, Labex Ecofect, 7 Passage du Vercors, 69367 Lyon, France

[2] Université de Lyon, Université Lyon 1, CNRS UMR 5246 Institut de Chimie et Biochimie Moléculaires et Supramoléculaires (ICBMS), Faculté de Pharmacie-ISPB, 8 Avenue Rockefeller, FR-69373 Lyon Cedex 08, France

[3] Department of Medicine II/Molecular Biology, University Hospital Freiburg, Medical Center, University of Freiburg, Freiburg 79106, Germany

[4] Physical Chemistry, ETH Zürich, 8093 Zürich, Switzerland

*Corresponding authors: lauriane.lecoq@ibcp.fr; thierry.lomberget@univ-lyon1.fr; anja.bockmann@ibcp.fr;

Materials and Methods

Molecular binders

Commercial compounds (**1a, b, c**; **2a, d**; **4a, b, c, f, g**; **6d, g**) were purchased from Sigma Aldrich. The synthesis of the other compounds used is described in the chemical syntheses annex of the Supplementary Information. Stock solutions of commercial and *de novo* compounds were prepared by diluting commercial solution or powder in DMSO, and then in the same buffer as the protein sample (except compounds **1a**, **1b** and **6g** which were directly diluted in protein's buffer). The typical concentration of the stock solutions was at 10 mM, and then the final solutions were calculated according to the experiments made, *i.e.* for ITC, the ligand should be at least 10 times more concentrated than the protein. For the final concentrations, it was established that the DMSO concentration should not exceed 5 % for either NMR or ITC experiments.

Expression and purification of Cp149

Plasmids of pET-28a2-HBc149opt were transformed into *E. coli* BL21*CP cells and grown at 37 °C overnight in 5 mL LB minimal medium culture, in presence of chloramphenicol and kanamycin. Precultures were diluted to yield a 1 L culture, and cells were grown at 37 °C until the optical density at 600 nm (OD_{600}) reached 0.6. Expression of Cp149 was then induced with

1 mM IPTG overnight at 20 °C. Cells were collected by centrifugation at 6,000 × g for 20 min and resuspended in 12 mL TN300 buffer (50 mM TRIS at pH 7.5, 300 mM NaCl, 2.5 mM EDTA, 5 mM DTT). During 1 h, the cell suspensions were incubated on ice with 1 mg/mL chicken lysozyme, 1X protease inhibitor mixture solution, and 0.5% Triton X-100 (TX100). Then, a total of 6 µL benzonase nuclease (0.5 µL/mL of protein solution) was added to digest nucleic acids for 45 min at room temperature. Cells were broken by sonication using a minimum of 10 cycles of 15 sec of sonication and 50 sec of cooling down on ice. Cell lysates were centrifuged at 30,000 g for 30 min to remove cell debris. The supernatant was loaded onto a 10 to 60 % sucrose gradient buffered with TN buffer and centrifuged in SW-32Ti Beckman Coulter swinging bucket rotor at 141,800 g for 3 h at 4 °C. Capsids in gradient fractions were identified by 15 % sodium dodecyl sulfate (SDS)-polyacrylamide gel. Then, proteins were precipitated by 35 % saturated ammonium sulfate (AS) during 30 min incubation and were centrifuged at 20,000 g for 40 min. Pellets were resuspended in 10 mL purification buffer (50 mM TRIS pH 7.5, 5 % sucrose, 5 mM DTT, and 1 mM EDTA). The proteins were centrifuged again for 20 min at 14,000 g to remove insoluble impurities. The capsids were dialyzed in purification buffer to remove remaining AS. Labelled proteins were expressed following the same protocols as unlabelled ones, except that those bacteria were grown in M9 minimal medium (with D_2O instead of H_2O) containing ^{13}C-deuterated glucose and $^{15}NH_4Cl$, and the induction was made at 25 °C.

Capsid disassembly and reassembly in vitro

Capsids were dialyzed overnight against disassembly buffer (50 mM $NaHCO_3$ pH 9.6, 5 mM DTT) at 4 °C. Capsid disassembly into dimers was achieved by the addition of urea powder at a final concentration of 3 M incubated overnight at 4 °C. To separate the dimers from remaining aggregates, size exclusion chromatography (SEC) was performed using a HiPrep 16/60 Sephacryl S-200 HR column (120 mL dead volume), previously equilibrated in disassembly buffer. The protein sample was filtered with a 0.45 µm PVDF membrane, before its injection on the column. The SEC also allows to remove TX100 from the hydrophobic pocket of the core protein.[1] Fractions containing dimers were pooled and concentrated with an Amicon (10,000 MWCO). For solution NMR experiments, Cp149 dimer solution was dialyzed in 50 mM HEPES buffer at pH 7.5, 5 mM DTT and directly used. Cp dimer samples were always controlled using negative staining electron microscopy (EM) to ensure the absence of capsids before running solution NMR experiments. For ITC and solid-state NMR, the dimer solution was dialyzed in reassembly buffer (50 mM TRIS pH 7.5, 500 mM NaCl, 5 mM DTT) overnight at 4 °C. The resulting reassembled capsids were checked by EM and finally dialyzed in 50 mM HEPES buffer at pH 7.5.

Solution NMR

Freshly prepared ^{2}H-^{13}C-^{15}N Cp149 dimer in 50 mM HEPES buffer (pH 7.5), 5 mM DTT was quantified by absorbance measurements, and concentrated to approximately 100 µM (in monomer concentration). The different compounds were added at a Cp-monomer:compound ratio of 1:4. Solutions were transferred into 3 mm solution NMR tubes, and ^{1}H-^{15}N SOFAST spectra were recorded on all samples on a 600 MHz spectrometer (Bruker Avance II) or 950 MHz spectrometer (Bruker Advance III) equipped with a triple-resonance cryo-probe. NMR

acquisition parameters are detailed in **Table S1**. The assignment from Cp149 dimer was transferred from BMRB deposition number 15969[2] and confirmed by 3D HNCO, HNCA and HNcoCA spectra recorded on the 950 MHz spectrometer on the control sample, since differences in the protein sequence and in pH did not allow a complete assignment transfer. New assignments were deposited in the BMRB under deposition number 51294. All spectra were recorded at 295 K and processed using TopSpin 4.0.8 (Bruker Biospin) and analyzed with the CcpNmr Analysis package, Version 2.4.2.[3] Chemical-shift perturbations (CSPs) between Cp149 dimer without and with ligand were calculated for each atom according to: $\Delta\delta_{HN} = \sqrt{(\Delta\delta_H)^2 + \left(\frac{\gamma_N}{\gamma_H}\Delta\delta_N\right)^2}$. A full CSP graph is shown for TX100 (**1a**) in **Figure S3**. For the other compounds, eight residues showing significant CSPs upon TX100 binding and isolated on the 2D spectrum were taken as representative probes: D2, I3, Y6, V13, L16, V27, T91 and T95. Average CSPs calculated on these 8 residues are detailed in **Table S2** for all compounds.

For the NMR titrations with TX100 (**1a**), OP (**1c**) and 4HF (**2a**) (, ^{2}H-^{13}C-^{15}N Cp149 dimer in 50 mM HEPES buffer at pH 7.5 and containing 5 mM DTT was quantified by absorbance measurements. ^{1}H-^{15}N SOFAST spectra were recorded for all ratios on the 600 MHz spectrometer (Bruker Avance II). NMR acquisition parameters are detailed in **Table S3**. For the titrations with TX100 (**1a**) and OP (**1c**), the protein was concentrated to approximately 140 µM (in monomer concentration) and 14 titration points were done from ratio 0 to 1.5 monomer:ligand. Titrations are shown in **Figure S5 and S6** (only 7 points are shown for clarity). For the titration with 4HF, ^{2}H-^{13}C-^{15}N Cp149 dimer was concentrated to approximately 80 µM (in monomer concentration) and four titration points were done at ratio 0, 0.5, 2 and 10 molar equivalents of monomer:ligand. Titration is shown in **Figure S7**. Stock solutions were done in HEPES buffer for TX100 and in 100 % DMSO for OP (**1c**) and 4HF (**2a**).

Solid-state NMR

For solid-state NMR, freshly prepared Cp149 reassembled capsids in 50 mM HEPES buffer (pH 7.5) were incubated with 4 to 8 equivalents of compounds to be investigated (TX100 (**1a**); OP (**1c**), and 4HF (**2a**)) for 2 hours at room temperature. They were then concentrated using Amicon Ultra centrifugal filter units (Merck, 50 kDa cut-off) to a concentration of about 20 mg/ml in 1 mL and sedimented into 3.2 mm zirconium rotors by ultracentrifugation (200,000 g, 14 h, 4 °C) using a home-made filling tool. Rotors were immediately closed after the addition of 1 µL of saturated DSS solution for chemical-shift referencing.

2D ^{13}C-^{13}C-dipolar assisted rotational resonance (DARR)[4] spectra were recorded using a 3.2 mm triple-resonance (^{1}H, ^{13}C, ^{15}N) wide-bore probe head at a static magnetic field of 18.8 T corresponding to 800 MHz proton resonance frequency (Bruker Avance II). All spectra were referenced to DSS and recorded at a sample temperature of 4 °C according to the resonance frequency of the supernatant water. Assignments were derived from those presented in [5] (bound-state) and [1] (unbound state). NMR acquisition parameters are detailed in **Table S4**. All spectra were processed using TopSpin 4.0.3 (Bruker Biospin) and analyzed with the CcpNmr Analysis package, Version 2.4.2.

Chemical-shift differences between Cp149 reassembled capsid without and with ligand were calculated for each carbon atoms according to: $\Delta\delta_C = \delta_C[bound] - \delta_C[unbound]$.

Isothermal calorimetry

Samples of freshly prepared Cp149 reassembled capsid were dialysed into 50 mM HEPES buffer at pH 7.5 and then quantified by absorbance measurements. ITC experiments were performed using a MicroCal iTC200 instrument (Malvern Panalytical, Malvern, Worcestershire, UK) at a temperature of 278 K. Briefly, binding enthalpies were obtained by injecting small volumes of compounds into the microcalorimeter reaction cell containing Cp149 reassembled capsid sample under stirring conditions (1,000 rpm) and a reference power of 5 µcal/s. In a typical ITC experiment, after a temperature equilibration delay, the measurement was started by a 1 µL injection of ligand (injection duration 2 s), followed by 15 injections of 2.5 µL (injection duration 5 s) in 2 min intervals. The heat evolution after each injection was obtained from the time integral of the calorimetric signal and the data were analysed assuming a single site binding model (one set of sites) using the MicroCal Origin software package. The thermodynamic parameters were calculated with the software provided by the instrument supplier. Control experiments for heats generated by mixing and dilution were performed under identical conditions and used for data correction in subsequent analysis.

Docking

Structure files of Cp149 dimer and OP (**1c**) ligand were prepared using MGLTools 1.5.6.[6] The initial PDB file of the ligand was obtained by extracting the TX100 (**1a**) coordinates from PDB structure 1UEH[7] and manually removing the hydrophilic tail. The ligand was set entirely flexible in the docking calculation, with four rotatable bonds. The coordinates of Cp149 were taken from PDB structure 1QGT [8], and mutation of residue 97 to Phenylalanine was introduced with USCF Chimera.[9] The receptor protein was prepared by selecting a search box encompassing the following residues showing large CSPs [1], that were also set flexibles: residues 1, 3, 6, 8, 27, 55, 58, 59 to 62, 64, 65, 68, 92, 93, 96 to 100 and 105 in one monomer and residues 42, 55, 58, 59, 60 to 62, 64, 65 and 68 in the other monomer, resulting in a total number of 69 rotatable bonds. The docking calculation was then performed using AutoDock Vina 1.1.2.[10] The resulting docked models were visualized with PyMoL (Delano W. L. http://www.pymol.org/).

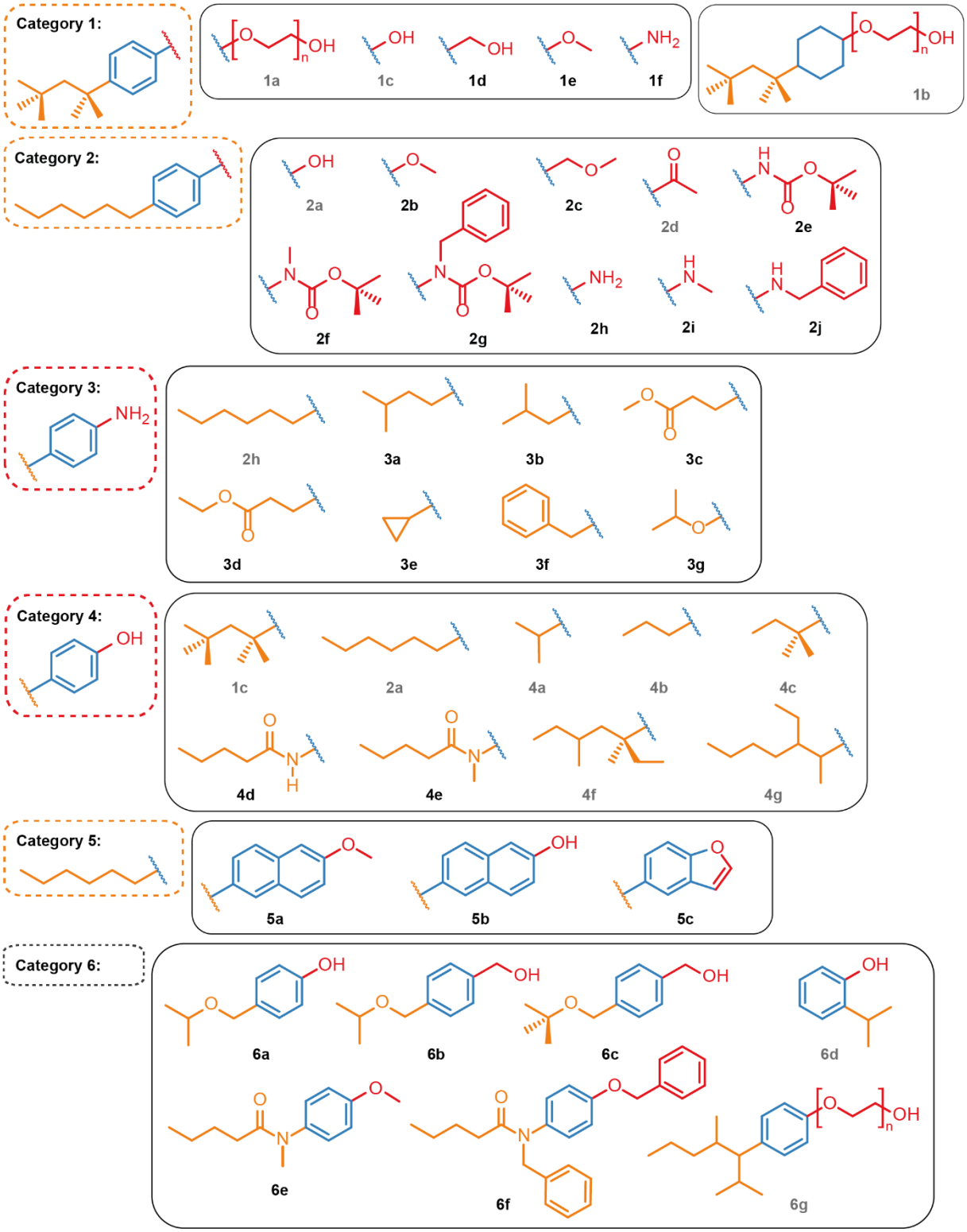

Figure S1. All molecules used in this study, categorized as a function of the moiety changed compared to Triton X-100, the compound of reference (**1a**). Commercial compounds are indicated with grey labels, and are: **1a**, Triton X-100 (TX100); **1b**, Reduced Triton X-100; **1c**, 4-*tert*-octylphenol (OP); **2a**, 4-hexylphenol (4HF); **2d**, 4'-heptylacetophenone; **2e**, 4-hexylaniline; **4a**, 4-isopropylphenol; **4b**, 4-propylphenol; **4c**, 4-*tert*-amylphenol; **4f**, 4-(3,5-dimethyl-3-heptyl)phenol; **4g**, 4-(2-ethyl-1-methylhexyl)phenol; **6d**, 2-isopropylphenol; **6g**, NP40.

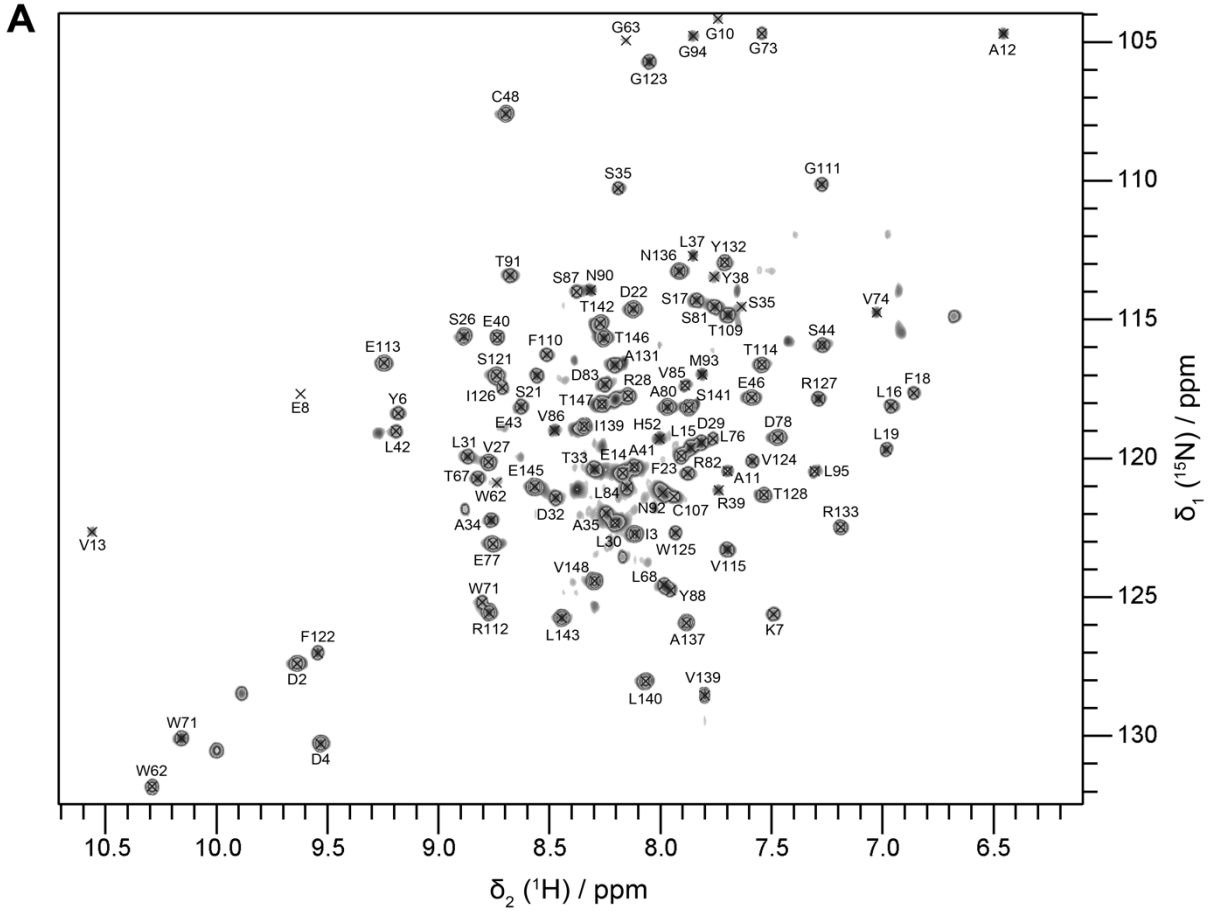

Figure S2. A) Solution-state NMR spectrum of the Cp149 dimer. B) Assignment reported on the sequence of Cp149. The residues of the hydrophobic pocket impacted by the interaction with TX100 (**1a**) are highlighted in blue. The eight residues whose NMR signals were used to quantify CSPs are highlighted in red, or purple if they are also part of the blue category, namely D2, I3, Y6, V13, L16, V27, T91 and L95. Unassigned residues are underlined. Resonance backbone assignments were deposited under BMRB accession number 51294.

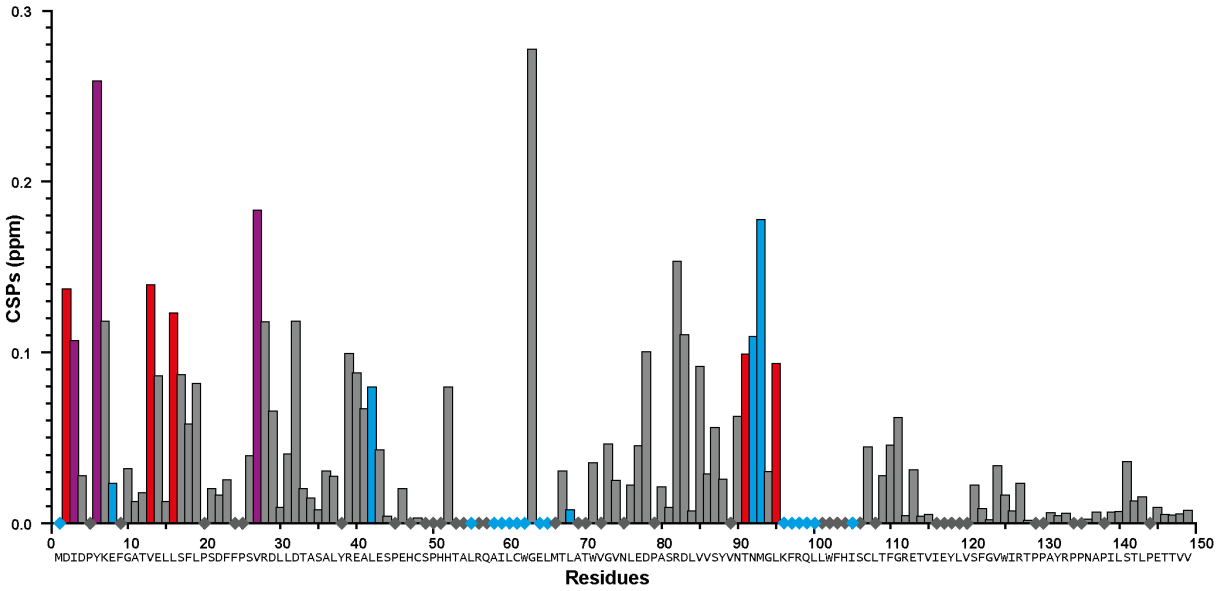

Figure S3. Full ^{1}H-^{15}N-CSP graph induced by TX100 (1a) on Cp149 dimer in solution-NMR. CSPs were calculated by comparing ^{1}H-^{15}N-BTROSY spectra of the ^{2}H^{13}C^{15}N-Cp149 dimer alone and with 4 molar equivalents of TX100 ([Cp149$_{monomer}$] = 80 µM and [TX100] = 320 µM). The unassigned residues are shown with a small diamond and are mainly due to incomplete amide back-exchange in the solvent-protected regions. The residues of the hydrophobic pocket the most impacted by the interaction of TX100 according to solid-state NMR data are highlighted in blue.[1] The eight residues used to establish binding efficiency are highlighted in red, or purple if they are also part of the blue category.

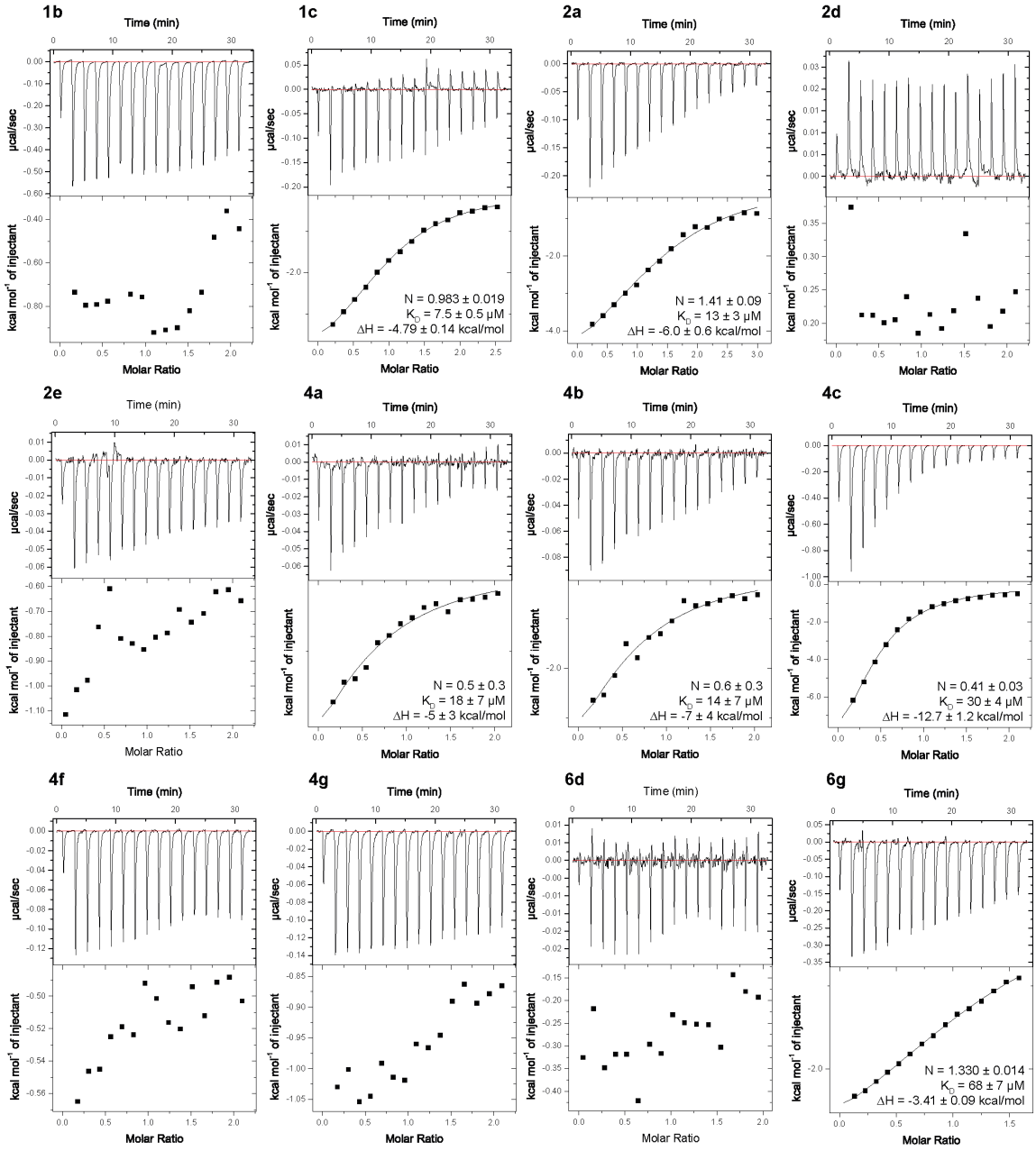

Figure S4. ITC raw data and binding isotherms obtained for Cp149 reassembled capsid upon additions of the indicated compounds. Experiments were done in 50 mM HEPES buffer at pH 7.5 and 298 K, with typical capsid concentrations of 100 µM ([$Cp149_{monomer}$]) and ligand concentrations of 1000 µM.

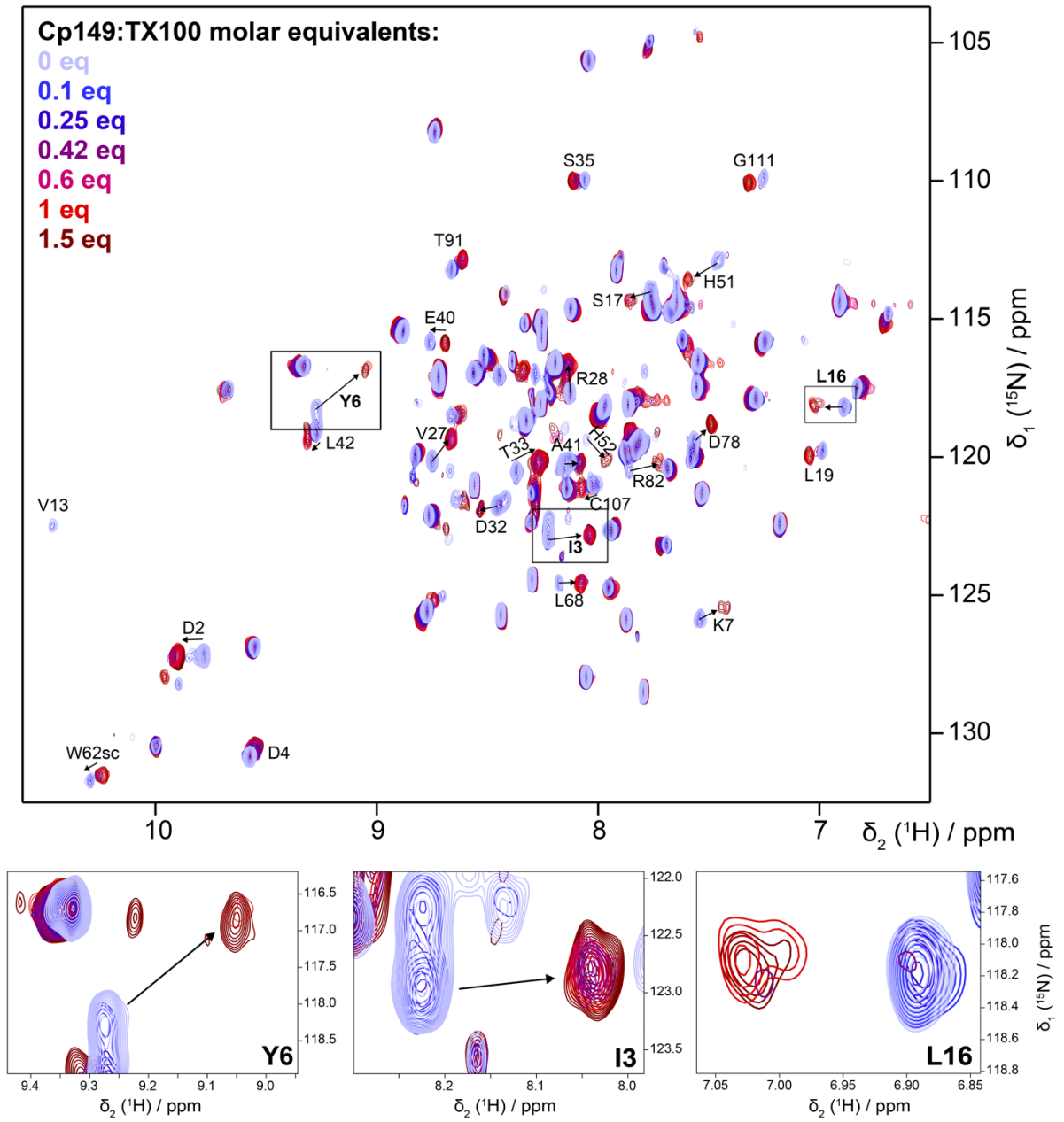

Figure S5. Titration of TX100 (**1a**) on Cp149 dimer ([$Cp149_{monomer}$] = 140 µM, from 0 to 1.5 molar equivalents monomer:TX100). The residues which move most are indicated by an arrow. A zoom is shown for residues Y6, I3 and L16. At the beginning of the titration (0, 0.2 and 0.5 equivalents, blue gradient spectra), the chemical shift observed corresponds to the free form and intensities start to decrease. Then, at 0.85 equivalents (purple spectrum), the signals broaden and in some cases are not visible (Y6), or the two forms are visible simultaneously (L16). Finally, above 1.2 equivalents (pink to brown spectra), the intensity of the signal corresponding to the bound form increases. The NMR line broadening is an indication that the interaction occurs in the slow-to-intermediate exchange regime, which usually occurs when the K_D becomes stronger than 10 µM.[11]

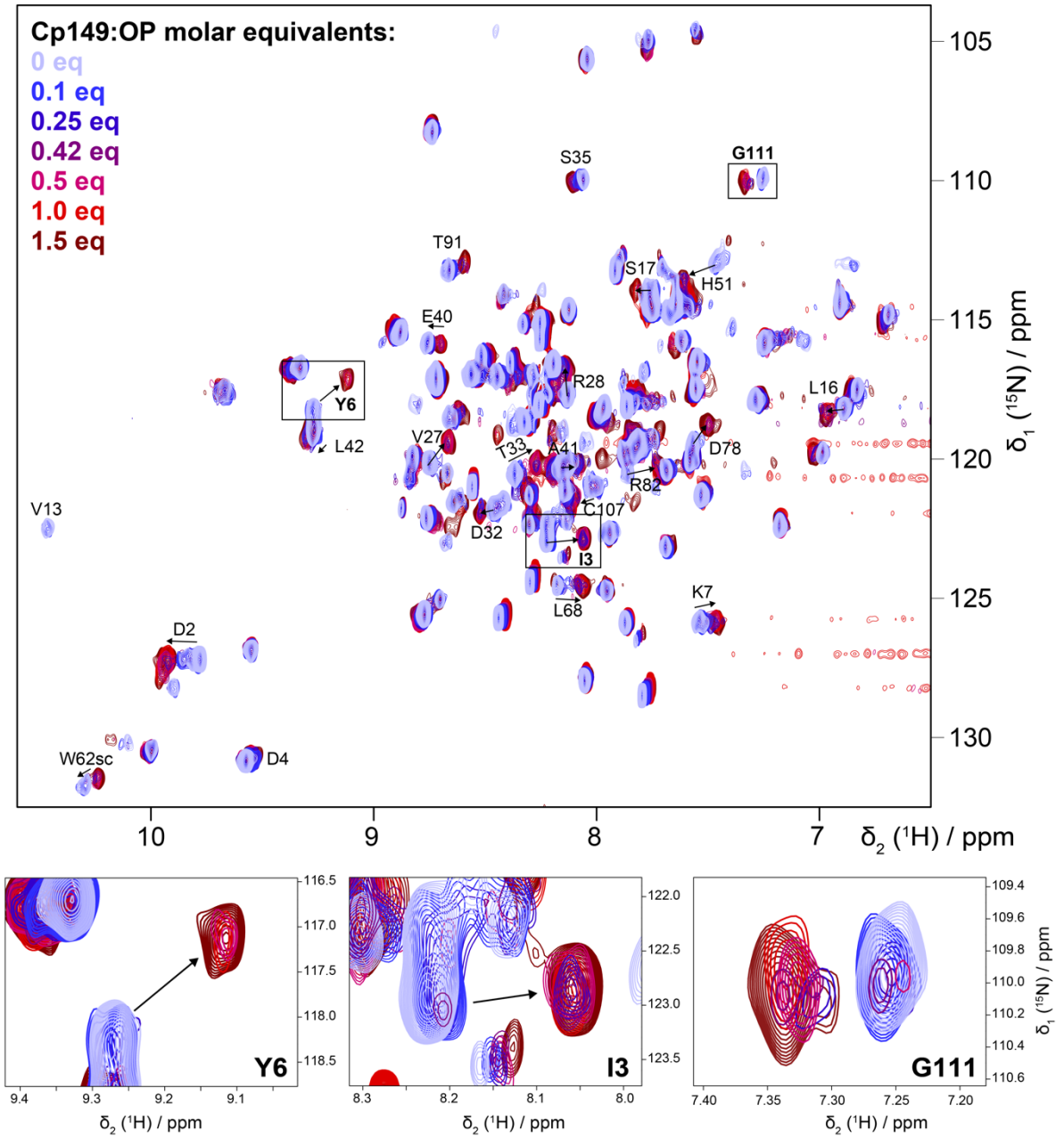

Figure S6. Titration of the Cp149 dimer with OP (**1c**) ([$Cp149_{monomer}$] = 140 µM, from 0 to 1.5 molar equivalents monomer:OP). The residues that move the most are indicated by an arrow. A zoom is shown for residues Y6, I3 and G111. The behaviour of the NMR signals is similar to what was observed upon titration with TX100 (**Figure S5**), corresponding to a slow exchange regime.

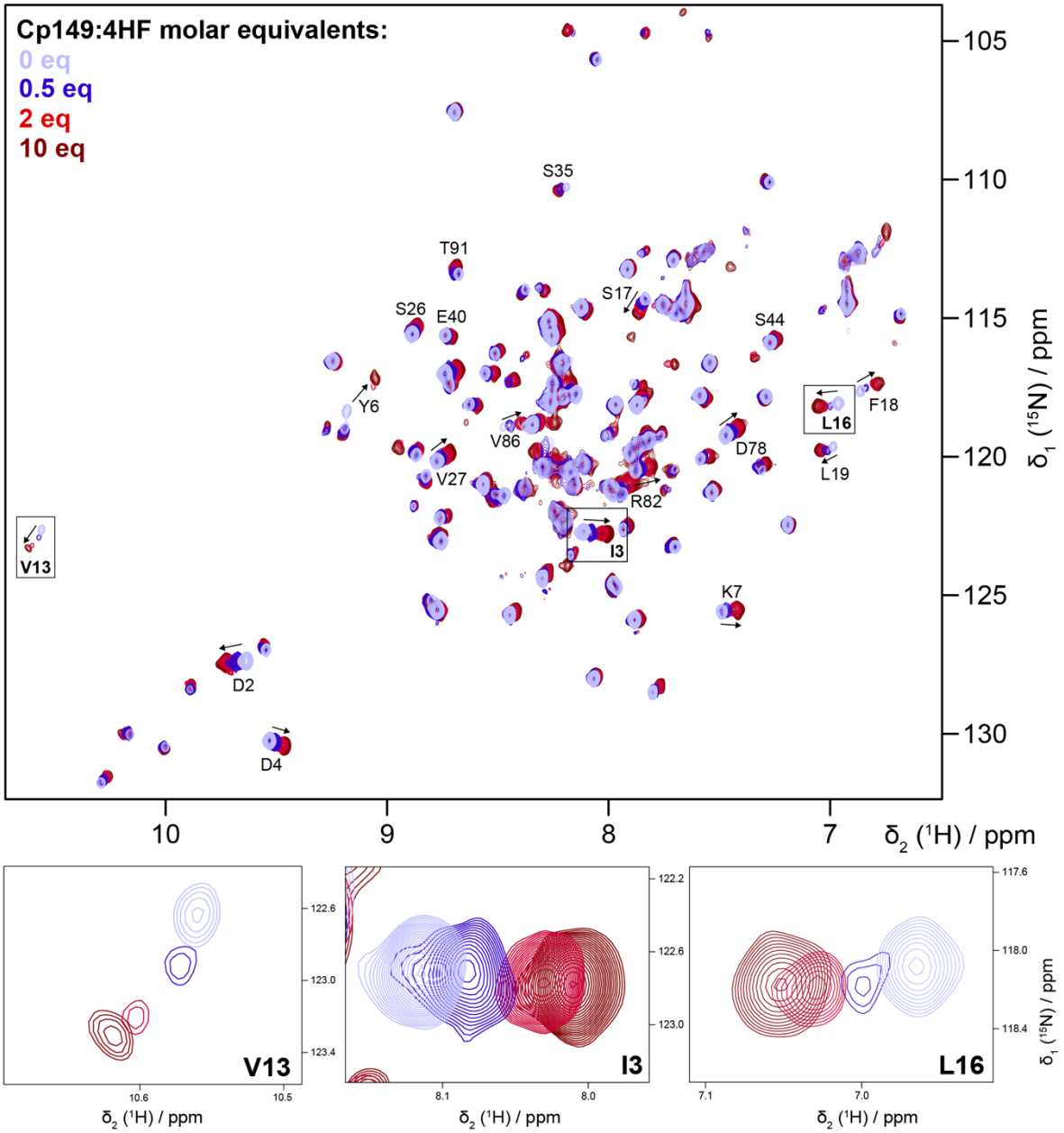

Figure S7. Titration of Cp149 dimer with 4HF (**2a**) ([$Cp149_{monomer}$] = 80 µM), from 0 to 10 molar equivalents monomer:4HF). The residues that move the most are indicated by an arrow. A zoom is shown for residues V13, I3 and L16. Contrary to TX100 and OP, here the titration indicates intermediate to fast exchange, where the observed chemical shift change is the weighted average of the shifts in the free and bound states.[11]

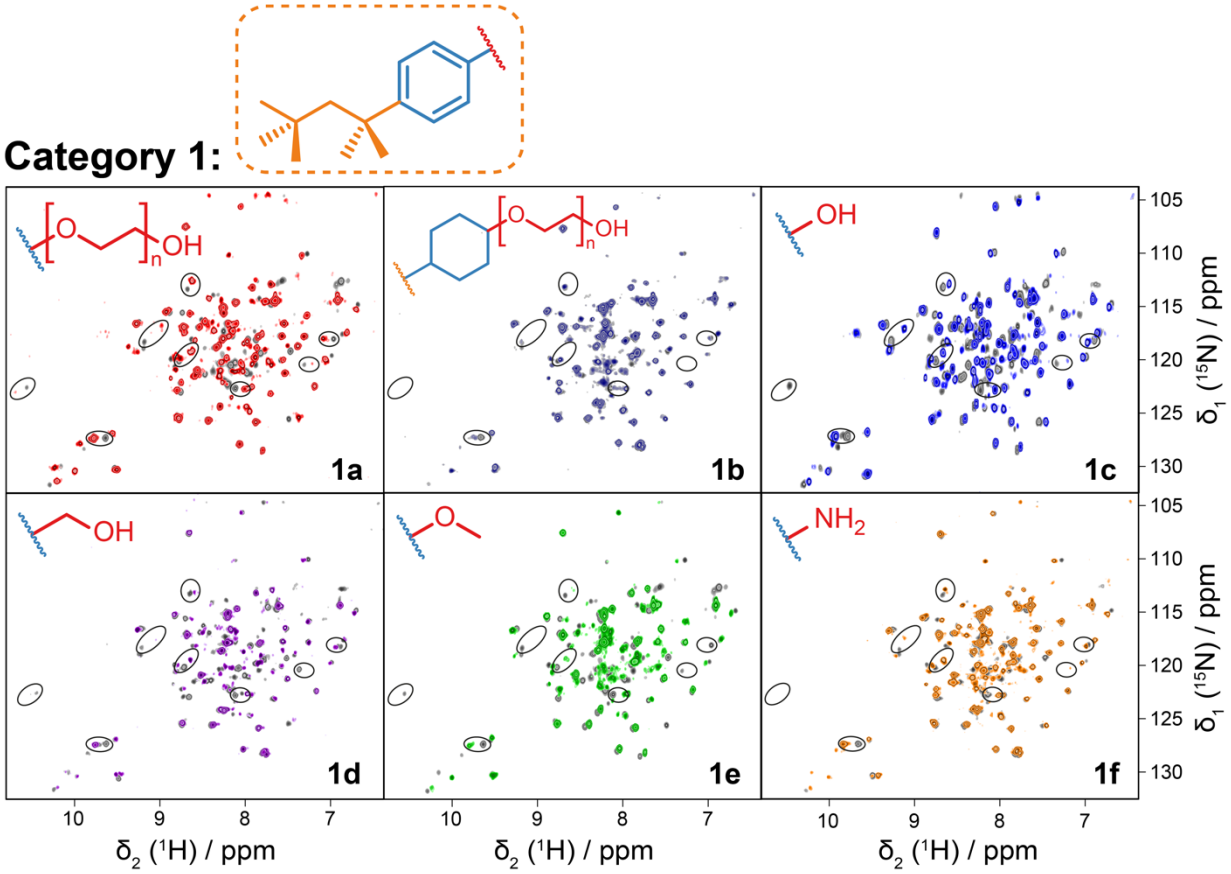

Figure S8. ^{1}H-^{15}N-HSQC spectra of the Cp149 dimer control (in grey) and in presence of 4 molar equivalents of compounds from the category 1 as displayed in **Figure S1**. The residues used for the determination of the interaction are circled. Note that control spectra may be different due to slight temperature changes coming from variable calibration from one spectrometer to another. Each spectrum recorded in presence of ligand is therefore overlayed with its corresponding control spectrum in light grey. Concentrations are for compound 1a, [$Cp149_{monomer}$] = 80 µM; compound 1d, [$Cp149_{monomer}$] = 90 µM; compounds 1b, 1f, [$Cp149_{monomer}$] = 120 µM; compound 1c[$Cp149_{monomer}$] = 120 µM.

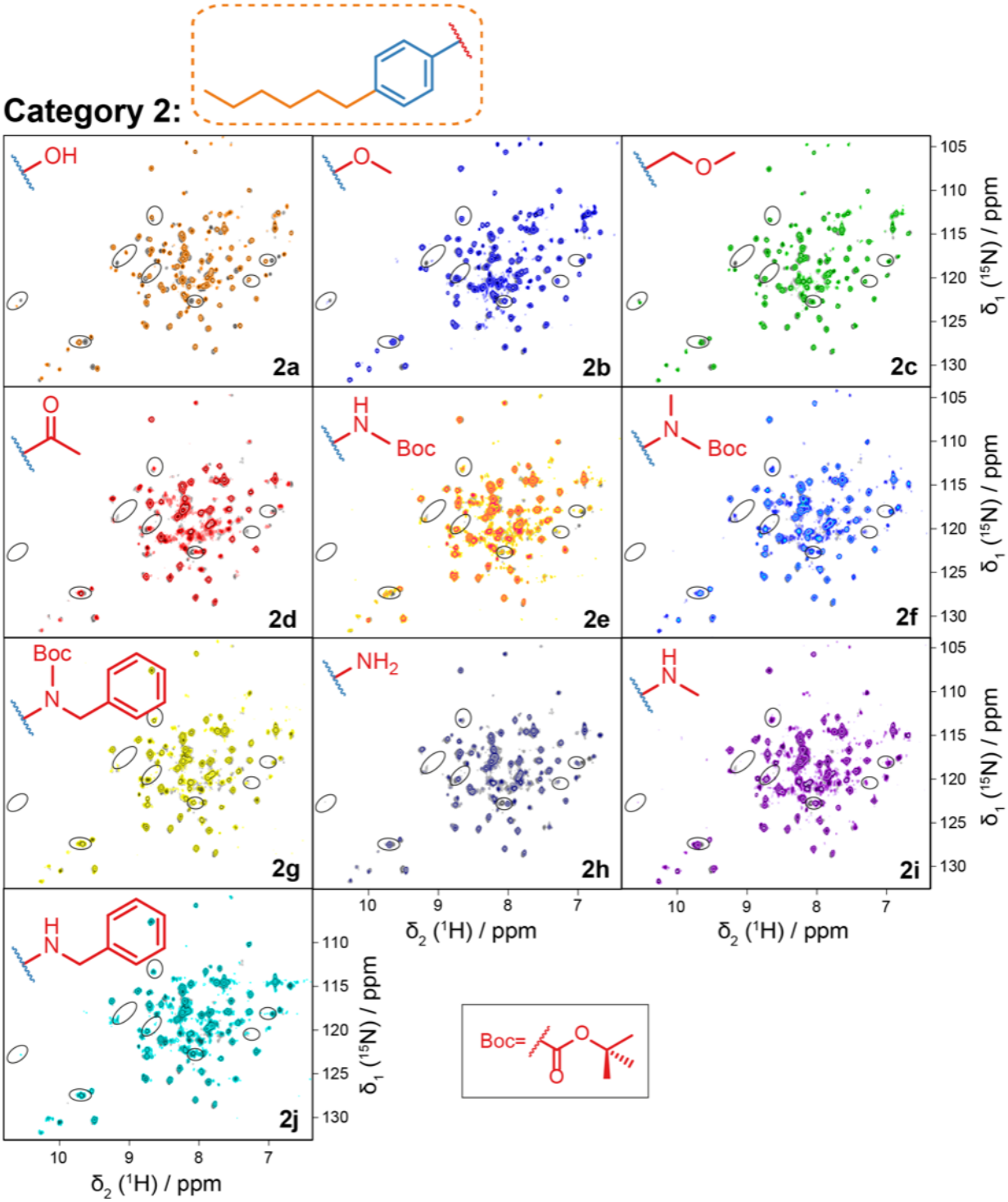

Figure S9. ^{1}H-^{15}N-HSQC spectra of Cp149 dimer control (in grey) and in presence of 4 molar equivalents of compounds from the category 2 as displayed in **Figure S1**. For compounds 2a, 2b, 2c, 2e, 2f, 2g, 2h, 2i, 2j, [$Cp149_{monomer}$] = 80 µM, and for compound 2d [$Cp149_{monomer}$] = 100 µM.

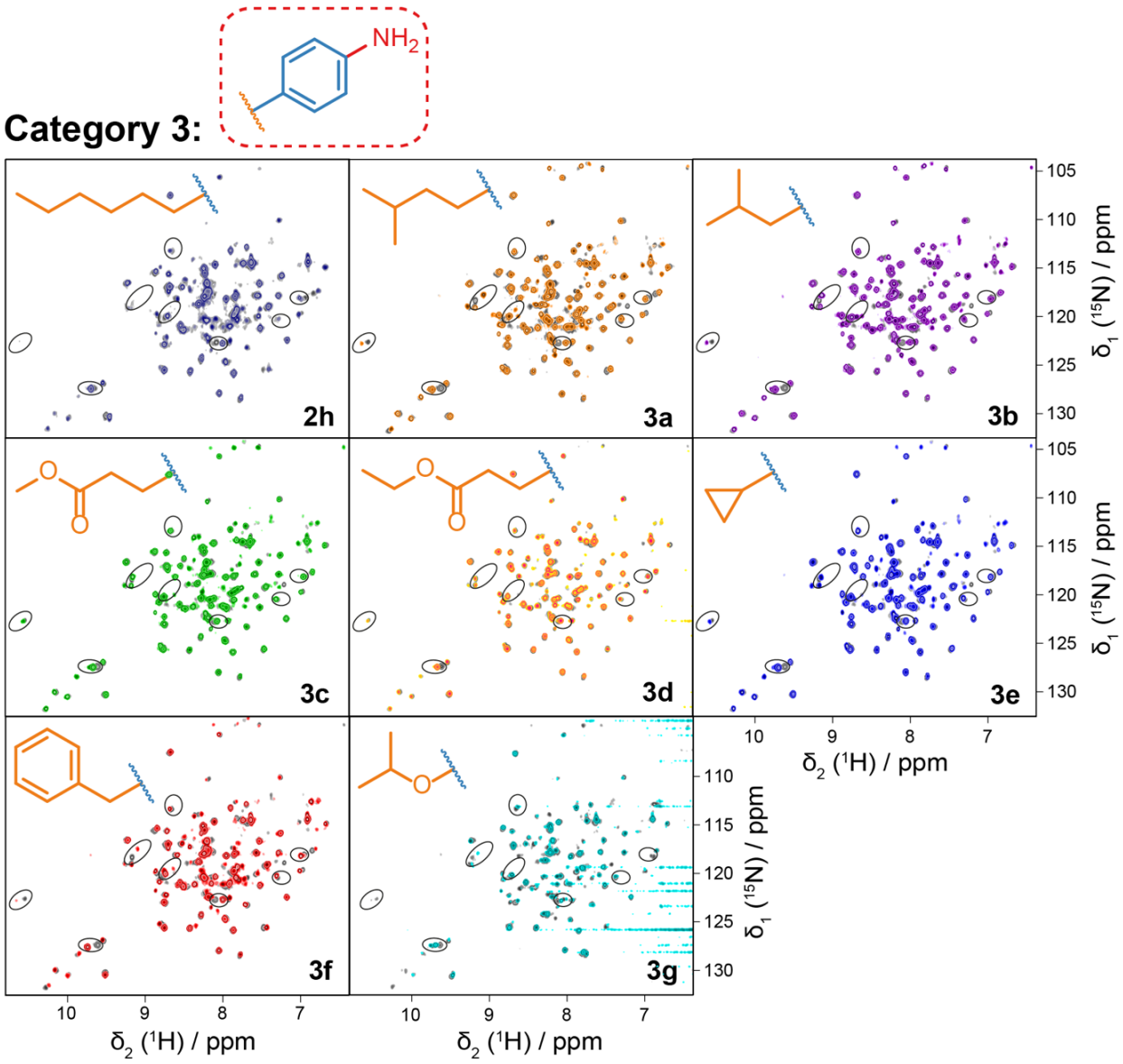

Figure S10. ^{1}H-^{15}N-HSQC spectra of Cp149 dimer control (in grey) and in presence of 4 molar equivalents of compounds from the category 3 as displayed in **Figure S1**. For compounds 3a, 3b, 3c, 3d, 3e, 3f, 3g, [$Cp149_{monomer}$] = 90 µM.

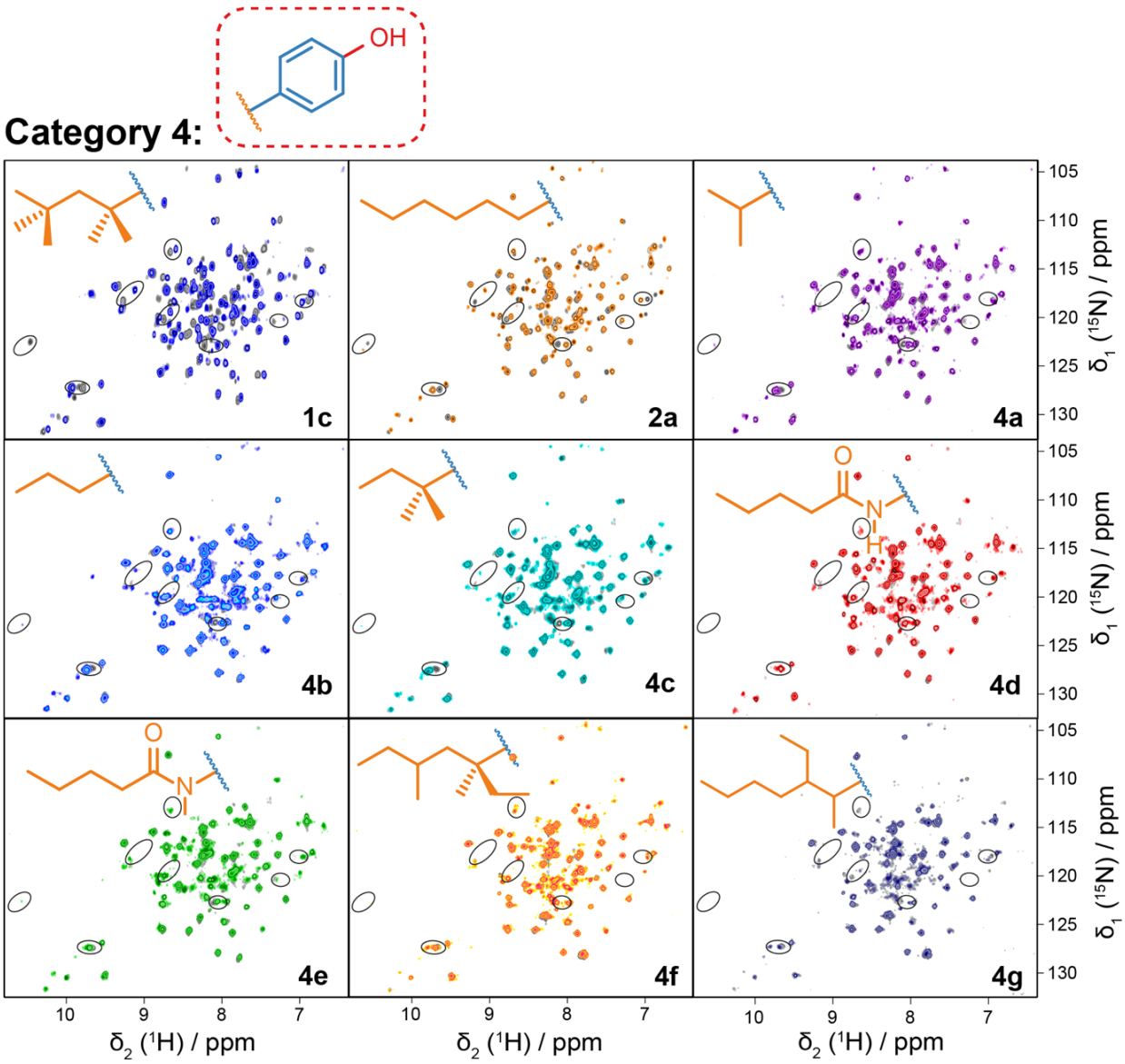

Figure S11. ^{1}H-^{15}N-HSQC spectra of Cp149 dimer control (in grey) and in presence of 4 molar equivalents of compounds from the category 4 as displayed in **Figure S1**. For compounds 4a, 4b, 4c, [Cp149 $_{monomer}$] = 100 µM; for compounds 4d, 4e, [Cp149 $_{monomer}$] = 80 µM; for compounds 4f, 4g, [Cp149 $_{monomer}$] = 120 µM.

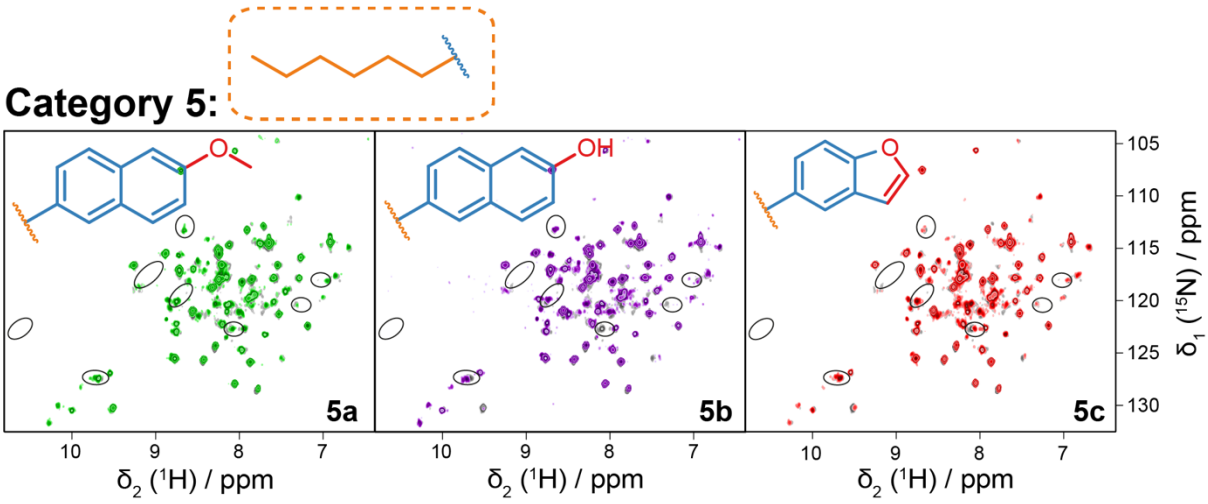

Figure S12. ^{1}H-^{15}N-HSQC spectra of the Cp149 dimer control (in grey) and in presence of 4 molar equivalents of compounds from the category 5 as displayed in **Figure S1**. For compounds 5a, 5b, 5c, [Cp149 $_{monomer}$] = 80 µM.

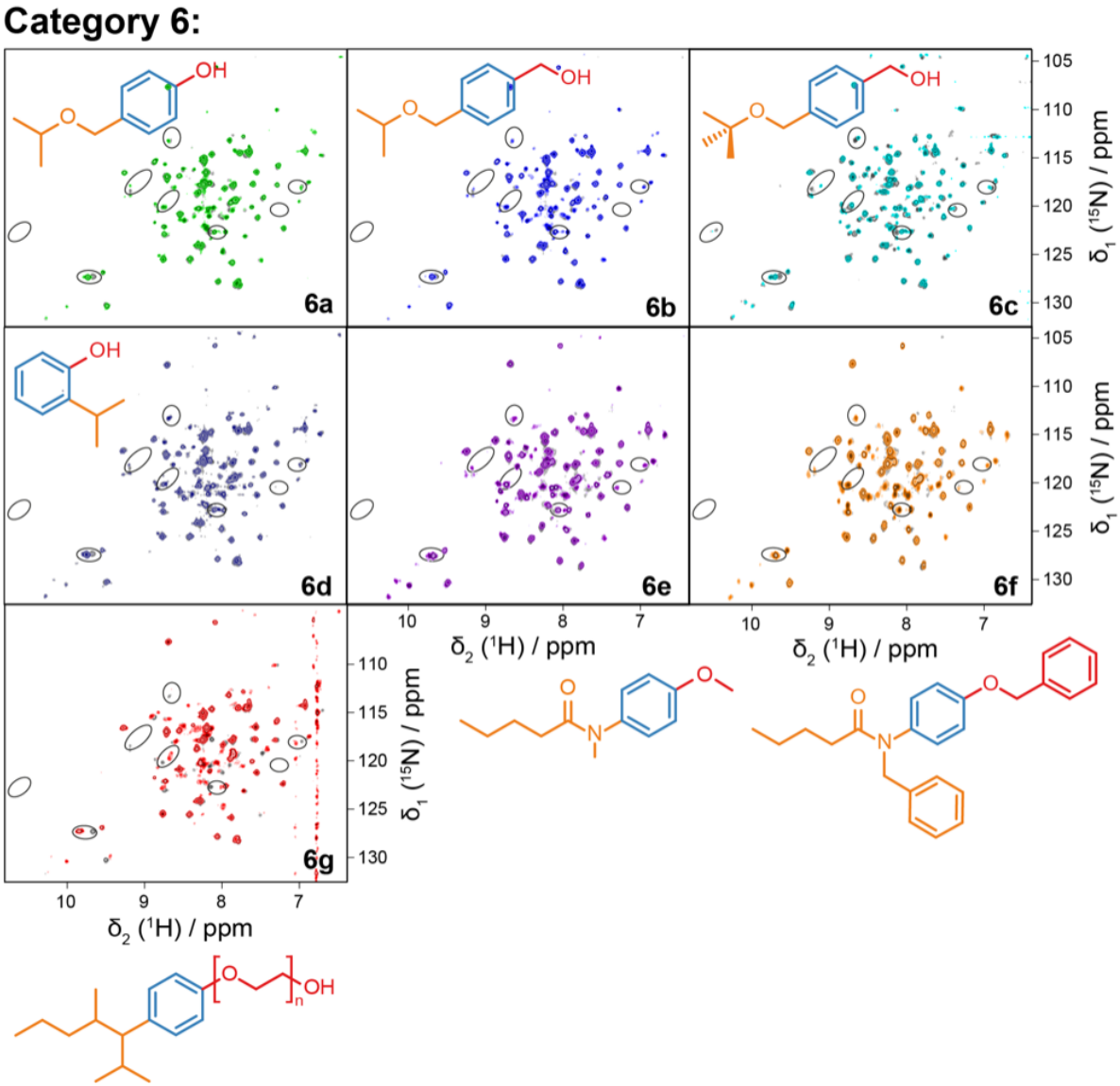

Figure S13. ^{1}H-^{15}N-HSQC spectra of the Cp149 dimer control (in grey) and in presence of 4 molar equivalents of compounds from the category 6 as displayed in **Figure S1**. For compounds 6a, 6b, 6d, 6g, [Cp149 $_{monomer}$] = 120 µM; for compound 6c, 6e, 6f, [Cp149 $_{monomer}$] = 80 µM.

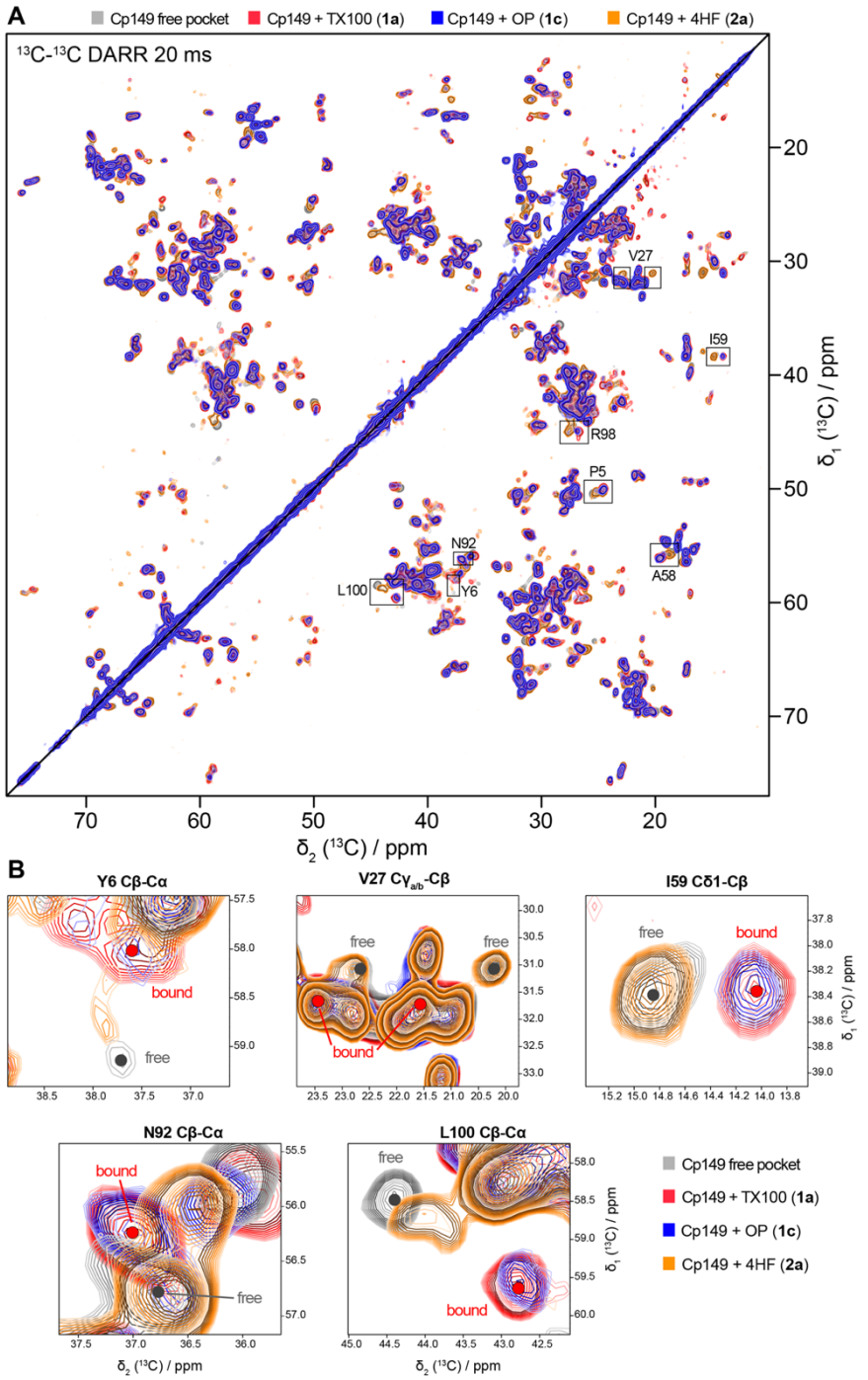

Figure S14. A) Comparison of the aliphatic region of 2D ^{13}C-^{13}C-DARR solid-state NMR spectra of Cp149 capsids reassembled in absence of compounds (empty pocket, in grey), Cp149 capsids reassembled with TX100 (**1a**, bound pocket, in red), with 4-*tert*-octylphenol (OP (**1c**), in blue) and with 4-hexylphenol (4HF (**2a**), in orange). B) Extracts of 5 correlation peaks from the 2D DARR spectra. Extracts for P5, A58 and R98 are shown in the main text in Figure 6, together with the CSPs.

Table S1. NMR experimental details of solution NMR measurements recorded on $^{2}H^{13}C^{15}N$-Cp149 dimer. sw stands for spectral width. 3 mm tubes were used for all recordings. Final percentage of DMSO varied from 0 to 5 %. The concentration is given for the monomer unit.

Ligand	**[Cp149] (µM)**	**Field (MHz)**	**sw {^{15}N} (ppm)**	**Increments {^{15}N}**	**Number of scans**	**Exp. time**
Control	140	600	29	100	24	12 min
1c	140	600	29	100	24	12 min
Control	80	600	29	200	64	1h08
1a, 1e, 2a, 2b, 2c, 2d, 2e, 2f, 2g, 2h, 2i, 2j, 4a, 4b, 4c, 4d, 4e, 5a, 5b, 5c, 6e, 6f	80	600	29	200	64	1h08
Control	100	600	29	200	48	51 min
3a, 3b, 3c, 3d, 3e, 3f	100	600	29	200	48	51 min
Control	100	600	29	200	64	1h08
1d, 6c, 3g	100	600	29	200	64	1h08
Control	120	950	29	316	64	1h38
1b, 1f, 4f, 4g, 6a, 6b, 6d, 6g	120	950	29	316	64	1h38

Table S2. Average CSPs calculated on the eight residues (D2, I3, Y6, V13, L16, V27, T91 and T95) for all compounds.

Category 1:

Compound	1a	1b	1c	1d	1e	1f
Average CSPs (ppm)	0.143	0.024	0.142	0.090	0.077	0.103
Standard deviation (Stdev, ppm)	0.018	0.007	0.017	0.018	0.017	0.018

Category 2:

Compound	2a	2b	2c	2d	2e	2f	2g	2h	2i	2j
Average CSPs (ppm)	0.083	0.029	0.031	0.029	0.020	0.008	0.014	0.052	0.030	0.014
Stdev (ppm)	0.016	0.009	0.009	0.004	0.004	0.002	0.003	0.009	0.006	0.002

Category 3:

Compound	2h	3a	3b	3c	3d	3e	3f	3g
Average CSPs (ppm)	0.052	0.064	0.052	0.021	0.016	0.029	0.072	0.035
Stdev (ppm)	0.009	0.015	0.015	0.006	0.006	0.009	0.016	0.009

Category 4:

Compound	1c	2a	4a	4b	4c	4d	4e	4f	4g
Average CSPs (ppm)	0.142	0.083	0.038	0.039	0.046	0.014	0.019	0.021	0.024
Stdev (ppm)	0.017	0.016	0.006	0.011	0.012	0.004	0.003	0.007	0.004

Category 5:

Compound	5a	5b	5c
Average CSPs (ppm)	0.009	0.027	0.016
Standard deviation (ppm)	0.002	0.004	0.004

Category 6:

Compound	6a	6b	6c	6d	6e	6f	6g
Average CSPs (ppm)	0.038	0.021	0.048	0.036	0.018	0.015	0.021
Standard deviation (ppm)	0.007	0.004	0.012	0.009	0.004	0.004	0.007

Table S3. NMR experimental details of solution NMR $^{1}H^{15}N$-SOFAST spectra recorded on $^{2}H^{13}C^{15}N$-Cp149 dimer for titration with TX100 (**1a**), OP (**1c**) and 4HF (**2a**). sw stands for spectral width. 3 mm tubes were used for all recordings. Final percentage of DMSO varied from 0 to 5 %. The concentration is given for the monomer unit.

Ligand	**[Cp149] (µM)**	**Field (MHz)**	**sw {^{15}N} (ppm)**	**Increments {^{15}N}**	**Number of scans**	**Exp. time**
TX100 (1a) and OP (1c)	140	600	29	100	24	12 min
4HF (2a)	80	600	29	100	64	33 min

Table S4. NMR experimental details of solid-state NMR measurements. sw stands for spectral width. Experiments were recorded on an 800 MHz wide-bore spectrometer at a 17.5 kHz MAS frequency and at a sample temperature estimated at 5 °C. The ^{15}N-insert was removed from the probe for the DARR experiments of samples with OP (**1c**) and 4HF (**2a**) to increase the signal-to-noise ratio. Experimental time for samples with Triton X-100 (**1a**) and with OP (**1c**) was longer to respectively compensate the fact that it was recorded with the ^{15}N-insert (TX100), and that the rotor was not full (OP).

Sample	**Cp149+TX100 (1a)**	**Cp149+OP (1c)**	**Cp149+4HF (2a)**
Experiment	2D DARR	2D DARR	2D DARR
Transfer 1	HC-CP	HC-CP	HC-CP
Field [kHz]	67.1 (^{1}H) 50 (^{13}C)	65.8 (^{1}H) 50 (^{13}C)	65 (^{1}H) 50 (^{13}C)
Shape	Tangent ^{1}H	Tangent ^{1}H	Tangent ^{1}H
^{13}C carrier [ppm]	58.6	58.6	58.6
time [ms]	0.8	0.7	0.9
Transfer 2	DARR	DARR	DARR
Field [kHz]	17.5(^{1}H)	17.5(^{1}H)	17.5(^{1}H)
^{13}C carrier [ppm]	100	100	100
time [ms]	20	20	20
t_1 increments	2560	2560	2560
sw (t_1) [kHz]	93.75	93.75	93.75
Acq. time (t_1) [ms]	13.7	13.7	13.7
t_2 increments	3072	3072	3072
sw (t_2) [kHz]	93.8	93.8	93.8
Acq. time (t_2) [ms]	16.4	16.4	16.4
^{1}H decoupling	SPINAL64	SPINAL64	SPINAL64
Field [kHz]	90	90	90
Interscan delay d1 [s]	2.6	2.6	2.6
Number of scans	20	20	8
Measurement time	38 h 40	38 h 40	15 h

References

[1] L. Lecoq, S. Wang, M. Dujardin, P. Zimmermann, L. Schuster, M.-L. Fogeron, M. Briday, M. Schledorn, T. Wiegand, L. Cole, R. Montserret, S. Bressanelli, B. H. Meier, M. Nassal, A. Böckmann, *Proc. Natl. Acad. Sci.* **2021**, *118*, e2022464118.

[2] S. M. V. Freund, C. M. Johnson, A. M. Jaulent, N. Ferguson, *J. Mol. Biol.* **2008**, *384*, 1301–1313.

[3] W. F. Vranken, W. Boucher, T. J. Stevens, R. H. Fogh, A. Pajon, M. Llinas, E. L. Ulrich, J. L. Markley, J. Ionides, E. D. Laue, *Proteins Struct. Funct. Bioinforma.* **2005**, *59*, 687–696.

[4] K. Takegoshi, S. Nakamura, T. Terao, *Chem. Phys. Lett.* **2001**, *344*, 631–637.

[5] L. Lecoq, S. Wang, T. Wiegand, S. Bressanelli, M. Nassal, B. H. Meier, A. Böckmann, *Biomol. NMR Assign.* **2018**, *253*, 80–10.

[6] G. M. Morris, R. Huey, W. Lindstrom, M. F. Sanner, R. K. Belew, D. S. Goodsell, A. J. Olson, *J. Comput. Chem.* **2009**, *30*, 2785–2791.

[7] S.-Y. Chang, T.-P. Ko, P.-H. Liang, A. H.-J. Wang, *J. Biol. Chem.* **2003**, *278*, 29298–29307.

[8] S. A. Wynne, R. A. Crowther, A. G. W. Leslie, *Mol. Cell* **1999**, *3*, 771–780.

[9] E. F. Pettersen, T. D. Goddard, C. C. Huang, G. S. Couch, D. M. Greenblatt, E. C. Meng, T. E. Ferrin, *J. Comput. Chem.* **2004**, *25*, 1605–1612.

[10] O. Trott, A. J. Olson, *J. Comput. Chem.* **2010**, 455–416.

[11] M. P. Williamson, *Progr NMR Spectr* **2013**, *73*, 1–16.